HEFAT2014
10th International Conference on Heat Transfer, Fluid Mechanics and Thermodynamics
14 – 16 July 2014
Orlando, Florida

THE CONTACT HEAT TRANSFER IN ROTARY KILNS AND THE EFFECT OF MATERIAL PROPERTIES

Nafsun A.I.[1]*, Herz F.[1], Specht E.[1], Scherer V.[2] and Wirtz S.[2]
*Author for correspondence
[1]Otto von Guericke University Magdeburg, 39106 Magdeburg, Germany
[2]Ruhr University Bochum, 44780 Bochum, Germany
E-mail: aainaa.nafsun@st.ovgu.de

ABSTRACT

This experimental work was conducted with different materials to study the influence of material properties on the contact heat transfer. The experimental study of conductive heat transfer between the covered wall surface and the solid bed has been investigated in an indirectly heated rotary drum with a diameter of D=0.6 m and a length of L=0.45 m. Temperature profiles of the gas, drum wall and solid bed were measured using 16 Type K thermocouples assembled on both a rotating and a fixed rod that attached inside the drum. Hence, the radial and circumferential temperature profiles were measured, and the contact heat transfer coefficients were calculated. Experiments have been carried out with six different materials including steel spheres, animal powder, cement clinker, quartz sand, glass beads and expanded clay. These materials have significantly different thermo physical properties (density, heat capacity and thermal conductivity) and particle diameters. The operating parameter, rotational speed, is varied by 1 and 6 rpm to evaluate the influence of rotational speed on the contact heat transfer coefficient in addition to the thermo physical properties and particle diameter. The measured contact heat transfer coefficients were compared with four model approaches from the literature. Good agreement between the experimental measurements and two model approaches were achieved.

INTRODUCTION

Rotary kilns are processing apparatuses used for drying, calcination or sintering in a variety of industries. Conditions in rotary kilns depend on the operational parameters (rotational speed, filling degree, material throughput, flow rate of gas/ solid), heating parameters (type of fuel, flame length and heat supply), design parameters (diameter, length and inclination angle) and the material parameters (particle size, particle shape, density, specific heat capacity, conductivity and dynamic angle of repose). The interaction of these parameters leads to a complexity in the rotary kiln processes. Hence, for safe design and process optimization, the process simulation is indispensable.

Rotary kilns can be heated directly or indirectly depending on the requirements of the processes. In indirectly heated rotary kilns, the contact heat transfer from the covered wall to the covered solid bed is dominant. Contact heat transfer also contributes up to 20% of the total amount of heat transfer to the solid bed in directly heated rotary kilns [2].

NOMENCLATURE

A_{WS}	[m²]	Contact surface area
$\alpha_{S,penetration}$	[W/m²/K]	Penetration heat transfer coefficient
α_{WP}	[W/m²/K]	Wall-Particle heat transfer coefficient
$\alpha_{WP,rad}$	[W/m²/K]	Radiation heat transfer coefficient
$\alpha_{WS,contact}$	[W/m²/K]	Heat transfer coefficient at the first particle layer
$\alpha_{WS,\lambda}$	[W/m²/K]	Contact heat transfer coefficient
$c_{p,S}$	[J/kg/K]	Solid specific heat capacity
d_P	[m]	Particle diameter
h	[m]	Bed height
L	[m]	Length of the drum
M_S	[kg]	Mass of the solid bed
R	[m]	Drum radius
$t_{contact}$	[s]	Contact time
T	[°C]	Temperature
λ_S	[W/m/K]	Solid bed conductivity
ρ_S	[kg/m³]	Solid bed density

Special characters

μ_P	[-]	Mean roughness on particle surface
F	[%]	Filling degree
l_G	[m]	modified free path of the molecules
n	[rpm]	Rotational speed
s_n	[mm]	Thermocouple distance
γ	[rad]	Filling angle
τ_W	[-]	Coverage factor

Subscripts

G	Gas
P	Particle
S	Solid
S,m	Mean solid bed
W	Wall

The contact heat transfer coefficient consists of a series of contact resistances between the wall and the particles and the penetration resistance inside the solid bed. The penetration resistance is influenced by the effective thermo physical properties of the solid bed. Therefore, it is important to study the influence of the thermo physical properties on the contact heat transfer.

Previous studies on the contact heat transfer have been done for monodisperse solid beds [1, 5, 6, 7, 8, 11, 16]. However, they did not address the influence of thermo physical properties on the contact heat transfer. Furthermore, there are numerous macroscopic models describing the contact heat transfer in literature [7, 11, 12, 13], but the quantitative predictions of these models are significantly different. Hence, this experimental work will be conducted with different materials to study the influence of material properties and particle diameter on the contact heat transfer and to show the quantitative differences between some existing models from the literature.

MODELLING OF THE CONTACT HEAT TRANSFER

Heat Transfer Mechanism and Motion Behavior

The heat transfer mechanism in rotary kilns includes conduction, convection and radiation. Figure 1 shows an indirectly heated rotary kiln. As the rotary drum wall, which is usually made of steel or graphite, is heated externally with $\dot{Q}_{\text{total}}$, heat from the source is transported to the wall and then conducted through the wall $\dot{Q}_{\text{W}}$. A part of heat radiates to the free solid bed surface $\dot{Q}_{\text{WS},\varepsilon}$ and the other part is conducted from the covered wall surface to the solid bed in the contact region, $\dot{Q}_{\text{WS},\lambda}$.

The covered and free surface of the wall and solid bed depends on the filling degree of the solid bed. The filling degree can be defined as the ratio of the cross sectional area of the solid bed to the total cross sectional area of the drum as shown in Figure 1. The geometric relation can be expressed as

$$\text{F} = \frac{\text{A}_{\text{solid bed}}}{\text{A}_{\text{drum}}} = \frac{\gamma - \sin\gamma\cos\gamma}{\pi} \quad \text{with } \gamma = \arccos\left(1 - \frac{h}{R}\right) \tag{1}$$

with the filling angle γ and the solid bed height h. In rotary kiln processes, rolling motion is desirable because it can realize perfect mixing of the solid bed. The motion behavior is influenced by the operational parameters (filling degree and rotational speed), design parameters (diameter and inclination angle) and material parameters. Typically, the filling degree used for industrial applications is in the range of 10% to 20%.

The rolling motion is described by the subdivision of the solid bed into two regions, the passive layer in the lower region and the active layer. These layers are separated by a fictitious boundary layer (ACB). In the passive layer, the particles are lifted up to the upper region due to contact with the wall during the rotation of the drum. At the upper boundary line (CA), the particles are mixed up into the active layer and flow down due to gravity along the line (AB). At the boundary line (BC), particles are mixed out of the active layer and mixed into the passive layer. This process occurs continuously; therefore, the solid bed is well mixed. Extensive experimental studies and modeling of the rolling motion were completed by Henein et al. [3, 4], Liu et al. [14] and Mellmann [15].

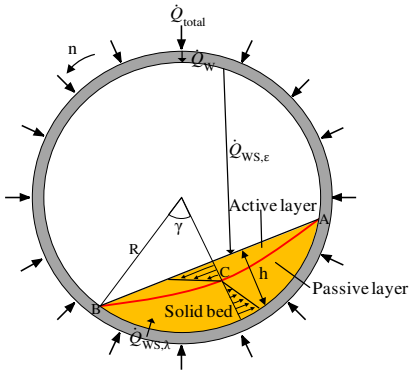

Figure 1 Schematic of the heat transfer in the cross section of indirect heated rotary kilns

Contact Heat Transfer

The contact heat transfer coefficient consists of the serial connection of the contact resistances between the wall and the particles $\alpha_{\text{WS,contact}}$ and the penetration coefficient inside the solid bed $\alpha_{\text{S,penetration}}$ as described in Schlünder [10].

$$\alpha_{\text{WS},\lambda} = \frac{1}{(1/\alpha_{\text{WS,contact}}) + (1/\alpha_{\text{S,penetration}})} \tag{2}$$

Due to the contact resistance, a high temperature gradient between the wall and the first particle layer occurs near to the wall, while the temperature decreases further into the solid bed because of the heat penetration resistance. The temperature further into the solid bed is defined as the average bulk temperature. By replacing the thermo physical properties of a particle (ρ_{P}, c_{P}, λ_{P}) with the effective properties of a bulk bed (ρ_{S}, $c_{\text{p,S}}$, λ_{S}), the bed can be regarded as a quasi-continuum. Assuming a constant wall temperature, the penetration coefficient is then obtained from Fourier's differential equation with

$$\alpha_{\text{S,penetration}} = 2\sqrt{\frac{\rho_{\text{S}}\, c_{\text{p,S}}\, \lambda_{\text{S}}}{\pi t_{\text{contact}}}} \qquad t_{\text{contact}} = \frac{\gamma}{\pi n} \tag{3}$$

where the contact time depends on the filling degree and the rotational speed. A notational gas layer between the first particle layer and the wall surface was assumed, which substantially affected the heat transfer by contact depending on the particle size. Schlünder [9] provided a physical justification for this process. It was expected that, near to the point of contact between the particles and the wall, a gas gap occurs in which the mean free path of the gas molecules is always greater than the thickness of this gas gap. Therefore, to compute the contact resistance between the bed and the wall surface, the conduction and radiation in the gas gap between the particles and the wall have to be considered in accordance with

$$\alpha_{\text{WS,contact}} = \tau_{\text{W}}\alpha_{\text{WP}} + \left(1 - \tau_{\text{W}}\right)\frac{2\lambda_{\text{G}}/d_{\text{P}}}{\sqrt{2} + 2\left(l_{\text{G}} + \mu_{\text{P}}\right)/d_{\text{P}}} + \alpha_{\text{WP,rad}} \tag{4}$$

This correlation was given by Schlünder and Mollekopf [11]. The second term in Eq. (4) describes the heat conduction to the second particle layer of the solid bed. The other variables are: α_{WP} and $\alpha_{WP,rad}$, the heat transfer coefficients by conduction and radiation in the gas gap between the first particle layer and the wall; τ_W the porosity dependent surface coverage factor; λ_G the conductivity of the gas in the gap; d_p the particle diameter; μ_P the mean roughness on the particle surface and l_G the modified free path of the molecules.

Wes et al. [13] investigated the contact heat transfer in an indirectly heated pilot plant (L = 9 m / D = 0.6 m). Within the experimental test series, maximum rotational speeds of n = 6.5 rpm were realized, so that the measurement results could be correlated with the penetration theory according to Eq. (3). Tscheng et al. [12] summarized the results of Wachters and Kramers [16] and Lehmberg et al. [6]. The model by Tscheng et al. [12] used a theory of a fictitious gas film between the wall surface and the first particle layer. A listing of the various models for the contact heat transfer in rotary kilns was provided by Li et al. [7]. Furthermore, a simplified model for the contact heat transfer based on [11] was developed.

EXPERIMENTS

Experimental Setup and Test Materials

A batch rotary drum was used in the experiments for the investigation of contact heat transfer as illustrated in Figure 2. It is a cylindrical drum made of steel with a wall thickness of 2 mm, an inner diameter of 600 mm and length of 450 mm. The drum was partially closed on both sides to prevent spillage of material. It is heated indirectly using three electric heaters with a total capacity of 4.5 kW, sufficient to reach a maximum temperature of 200°C. The test material was heated up from ambient temperature to steady-state conditions using a constant heat flux from the outer heating system. The temperature of the inner wall, air and solid bed were measured by thermocouples installed to the drum. The signals from the thermocouples were sent to the data acquisition system and analyzed.

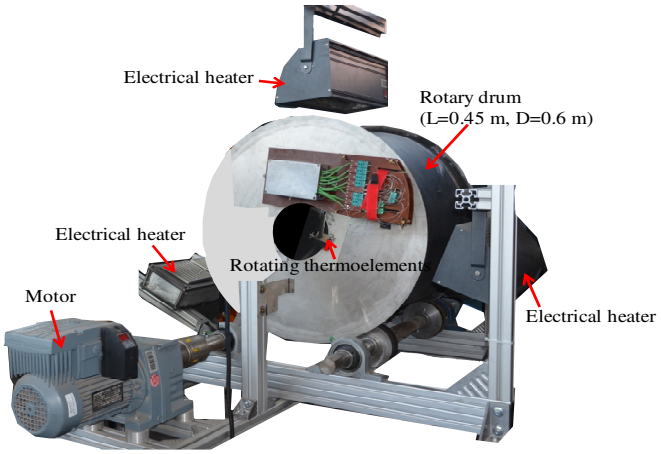

Figure 2 The batch rotary drum for the investigation of contact heat transfer coefficient

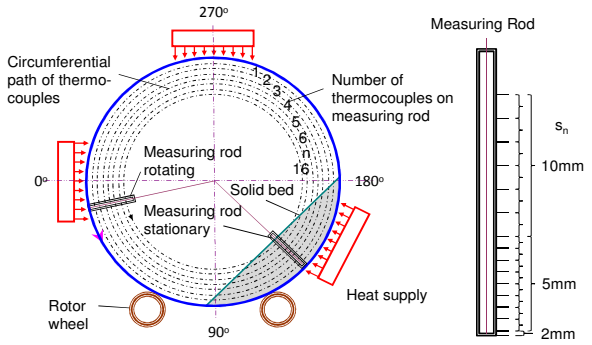

Figure 3 Schematic cross section of the batch rotary drum and thermocouples arrangement.

The temperature inside the drum was measured by 15 thermocouples attached to a rotating rod at specific distances from the inner drum wall as shown in Figure 3. With this rotating rod, the radial temperature as well as the circumferential temperature profile of the solid bed could be measured simultaneously. In addition, one thermocouple was installed directly on the surface of the inner wall of the drum to simultaneously measure the wall temperature of the drum. Hence, overall 16 thermocouples were used to measure the temperature inside the drum. These thermocouples are Type K thermocouples, made of NiCr-Ni with a diameter of 0.5 mm. Another stationary measuring rod was installed and positioned in the solid bed at a 130° circumferential position. This stationary measuring rod was used to assess the delay of the thermocouples at the rotating rod. 16 thermocouples were attached on this rod with the same radial spacing of the rotating rod. The rotating and fixed rods are located at 200 mm and 250 mm in the axial position of the drum, respectively. Hence, the end wall effect to the contact heat transfer can be neglected. The temperature difference between the two measuring rods is considered to be negligible. This is because of the very low response time when the diameter of the thermocouples is very small. Therefore, the temperature measured by the rotating thermo elements is considered to have ample accuracy for the heat transfer calculation.

Table 1 Test materials and their properties.

Testing material	Steel spheres	Animal powder	Cement clinker	Expanded clay	Glass beads	Quartz sand
Particle diameter d_P (mm)	2.0	0.4	4.5	3.0	2.0	0.2
Bed density ρ_S (kg/m^3)	4827	574	1478	432	1680	1590
Specific heat capacity $c_{p,S}$ (J/kg/K)	465	1538	917	769	800	1080
Thermal conductivity λ_S (W/m/K)	1.37	0.12	0.20	0.12	0.25	0.30

The experiments were performed with a constant filling degree of F=20% and rotational speeds of 1 rpm and 6 rpm. Six different materials are used as a testing bed: steel spheres, animal powder, cement clinker, quartz sand, glass beads and expanded clay. The effective thermo physical properties and particle diameter of these materials are shown in Table 1.

Experimental Analysis

The measured circumferential temperature profiles for animal powder after 40 minutes experimental time are shown in Figure 4. The thermocouples distanced from the wall measured the air temperature inside the rotary drum initially from 0° to 70° (not shown in the figure). At 71°, the thermocouples located nearest to the wall immersed earliest into the solid bed and were followed by the next adjacent thermocouples. The rise in temperature was initially recorded by the thermocouple 2 mm from the wall at about 71° while the last thermocouple that recorded a temperature increase was the thermocouple 102 mm from the wall at 100°. The farthest thermocouple (102 mm) emerged from the bed earliest at about 164° while the nearest thermocouple (2 mm) to the wall emerged out of the bed lastly at about 200°. So it is clearly shown that the response time of the installed thermocouples is very small, as described before. As seen in Figure 4, a uniform temperature of the solid bed was obtained from 120° to 160°, but the temperature in the solid bed decreases with radial distance from the wall. The difference in the solid bed temperature depends on the radial position, so a surface-related mean temperature is used to calculate the heat transfer coefficient with

$$T_{S,m}=\frac{A_1\left(\frac{T_W+T_1}{2}\right)+A_2\left(\frac{T_1+T_2}{2}\right)+\ldots.+A_n\left(\frac{T_{n-1}+T_n}{2}\right)}{A_1+A_1+\ldots..+A_n} \quad (5)$$

and

$$A_n = 2\left(R_{n-1}-s_n\right)\gamma L. \quad (6)$$

The contact heat transfer coefficient from the experimental study can be calculated using the energy balance equation. This was done by assuming that the total energy supplied from the wall was transferred to the solid bed. Heat losses to the surrounding were neglected because the wall temperature was measured directly at the inner wall of the drum. The enthalpy transport in the wall also was neglected due to the small wall thickness of 2 mm. The heat transfer coefficient was derived from the energy balance as follows:

$$\alpha_{WS,\lambda}\,A_{WS}\left(T_W-T_{S,m}\right)=M_S c_{p,S}\frac{dT_{S,m}}{dt} \quad \text{with} \quad A_{WS}=2\gamma RL \quad (7)$$

where $T_{S,m}$ is the mean temperature of the solid bed, T_W is the wall temperature and $c_{p,S}$ is the specific heat capacity of the solid bed. The mass of the solid bed M_S and the contact surface area A_{WS} are filling degree and solid material dependent measuring values that do not vary during the test series.

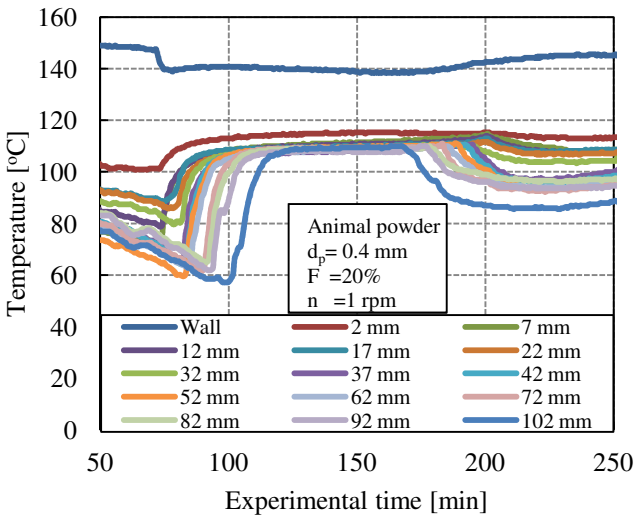

Figure 4 Circumferential temperature profiles of the wall and inside the solid bed (animal powder).

RESULTS AND DISCUSSION

Figure 5 shows the temperature profiles of the inner drum wall and mean solid bed for animal powder during the measurement. Initially, the temperature difference between the inner wall and mean solid bed is relatively large. After 100 minutes, the inner wall temperature begins to asymptotically reach steady state. Hence, the mean bed temperature converges to the wall temperature and the temperature difference between the inner wall and the mean solid bed reduces. The temperature gradient in the solid bed also reduces and has a tendency toward zero; hence, the contact heat transfer coefficient reduces.

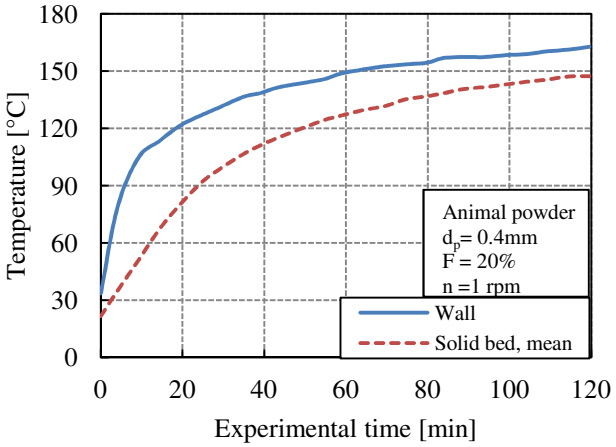

Figure 5 Time curve of the mean solid bed and inner wall temperature during the experiment (animal powder).

Figure 6 shows the distribution of the contact heat transfer coefficient for animal powder during the experiment. As the contact heat transfer coefficients are derived from the temperature measurement, they fluctuate due to the temperature fluctuation during the test. From these fluctuating values of the

heat transfer coefficient, a mean heat transfer coefficient was obtained. The deviation of the regression curve is in the range of 20%, which is represented by the error bars of the mean values in Figure 6. It can be seen that all the measured values are in the range of accuracy. The regression curve of the mean heat transfer coefficients were also formed for each set of experiments.

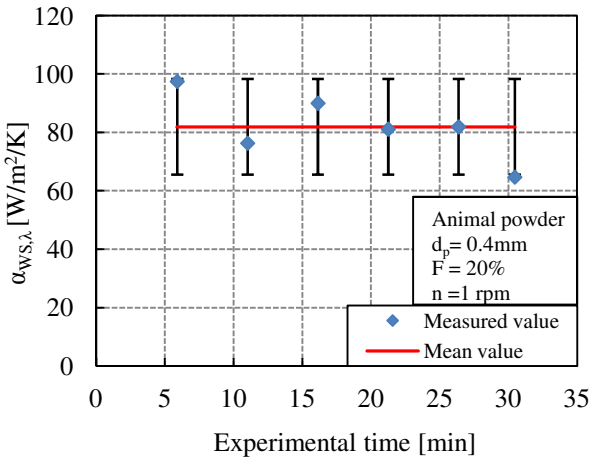

Figure 6 Time curve and regression deviation of the contact heat transfer coefficient during a test section (animal powder).

The influence of rotational speed on the contact heat transfer for animal powder is shown in Figure 7. The contact heat transfer coefficient increases with higher rotational speeds. As the rotational speed increases, the contact time between the covered wall surface and solid bed decreases. Accordingly, the penetration resistance decreases. Moreover, the number of bed circulations increases with higher rotational speeds thus promoting better mixing within the solid bed. The increase of the contact heat transfer with higher rotational speeds is qualitatively confirmed by the experimental measurement and the models by Wes et al. [13], Schlünder et al. [11], Li et al. [7] and Tscheng et al. [12]. However, these models show quantitatively large differences between them.

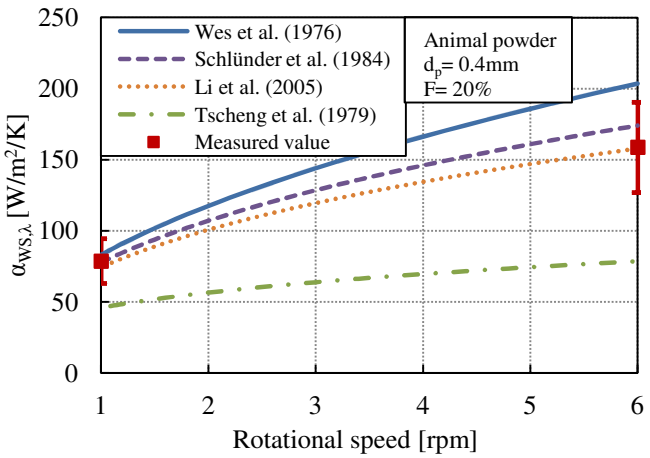

Figure 7 Contact heat transfer coefficient for animal powder in dependence on rotational speed.

As can be seen in Figure 7, the model by Li et al. [7] fits the experimental measurements very well since this model is appropriate for materials with particle diameters up to 1 mm. The model by Schlünder et al. [11] shows good agreement with the experimental measurement and lies within the range of accuracy. The model by Wes et al. [13] shows good agreement for lower rotational speeds, but it is away from the accuracy range for higher rotational speeds. The model by Tscheng et al. [12] shows significantly lower values of the contact heat transfer coefficient, which could not be validated. The assumption of a fictitious gas layer between the covered wall and the first particle layer caused a high contact resistance thus low contact heat transfer coefficients were obtained by using this model.

The comparisons of the contact heat transfer coefficient as a function of rotational speed for all the materials are shown in Figure 8. It can be seen that the contact heat transfer coefficients for all materials are significantly different from each other. This is due to the differences in particle diameter and effective thermo physical properties (bulk density, heat capacity and thermal conductivity) of the materials.

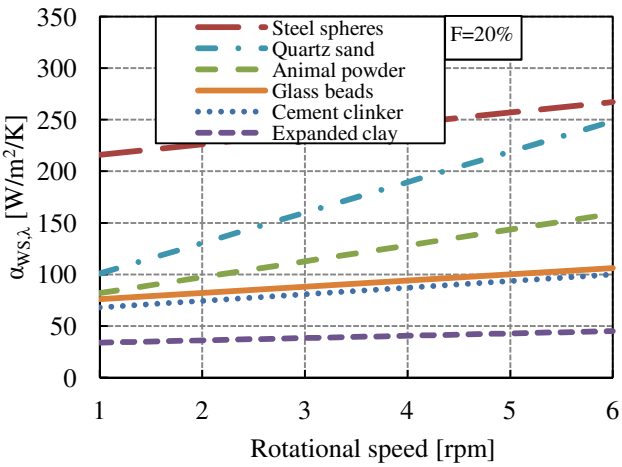

Figure 8 Contact heat transfer coefficient in dependence on rotational speed for different materials.

Steel spheres have the largest value of contact heat transfer coefficient. This is followed by quartz sand, animal powder, glass beads, cement clinker and expanded clay. Steel spheres have the highest values of effective bulk density and effective thermal conductivity compared to the other test materials. This causes the penetration resistance inside the solid bed to decrease, thus the highest contact heat transfer coefficients were obtained. On the other hand, expanded clay has the lowest values of effective bulk density and effective thermal conductivity. The penetration resistance inside the solid bed was high and the lowest contact heat transfer coefficients were obtained as illustrated.

As shown, cement clinker has a higher contact heat transfer coefficient than expanded clay. Cement clinker has an effective bulk density approximately 3.5 times higher, an effective thermal conductivity 1.8 times higher and an effective heat capacity 1.2 times higher than expanded clay. This reduces the

penetration resistance inside the solid bed thus producing a higher contact heat transfer coefficient. Although the particle diameter of cement clinker is 1.5 times higher than expanded clay, the effect of the particle diameter is offset by the effect of the thermo physical properties. In this case, the penetration resistance has a major influence on the contact heat transfer coefficient.

Glass beads have a slightly higher heat transfer coefficient than cement clinker. The thermo physical properties of these materials are nearly the same. On the other hand, the cement clinker has a particle diameter almost 2.3 times bigger than the glass beads. Hence, the contact resistance from the wall to the first particle layer is higher and results in a lower contact heat transfer coefficient compared to glass beads.

Animal powder has a higher contact heat transfer coefficient than glass beads, cement clinker and expanded clay. The particle diameter of animal powder is very small compared to these materials. It has a particle diameter about 12, 8 and 5.4 times lower than cement clinker, expanded clay and glass beads, respectively. In this case, contact resistance has a greater influence on the contact heat transfer coefficient than penetration resistance. As the particle diameter decreases, the contact resistance between the covered wall and the first particle layer also decreases. Hence, higher contact heat transfer coefficients were obtained.

Quartz sand has a higher contact heat transfer coefficient compared to animal powder. Both the thermo physical properties and particle diameter influence the contact heat transfer coefficient. Quartz sand has an effective bulk density 2.8 times higher and an effective thermal conductivity 2.5 times higher than animal powder. With higher thermo physical properties, the penetration resistance inside the solid bed reduces. Quartz sand also has a particle diameter about 2 times smaller than animal powder, thus the contact resistance between the wall and the first particle layer decreases. As a result, the contact heat transfer coefficient of quartz sand is higher than that of animal powder. All the values from the experimental measurement and models calculation are summarized in Table 2.

Four materials, expanded clay, cement clinker, glass beads and steel spheres, were chosen to show the influence of their thermo physical properties on the **c**ontact heat transfer coefficient. These materials were selected because their mean particle diameters are in the same range, and hence the effect of the contact resistance on the contact heat transfer coefficient is small and could be neglected.

Figure 9 shows the dependence of the contact heat transfer coefficient on the thermal conductivity of the solid bed. It can be seen that the contact heat transfer coefficient increases with higher effective thermal conductivities. A higher effective thermal conductivity promotes better heat penetration into the solid bed and reduces the penetration resistance. Consequently, the contact heat transfer coefficient increases.

Table 2 Contact heat transfer coefficient for all test materials from the experimental results and model calculations.

n [rpm]	$\alpha_{ws,\lambda}$ in W/m^2/K				
	Experim.	Wes et al.[13]	Tscheng et al.[12]	Schlünder et al.[11]	Li et al.[7]
Steel spheres					
1	173-259	440	326	177	101
6	213-320	1079	559	233	116
Animal powder					
1	65-98	83	46	78	74
6	127-190	204	79	174	158
Cement clinker					
1	54-82	132	74	70	40
6	80-120	323	126	102	49
Expanded clay					
1	27-41	49	33	40	31
6	36-54	120	56	76	50
Quartz sand					
1	81-122	106	48	101	98
6	198-298	260	83	229	217
Glass beads					
1	60-90	146	86	98	69
6	85-127	359	147	162	96

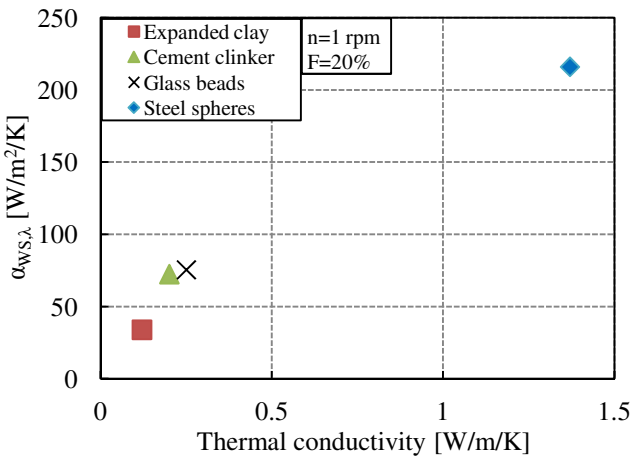

Figure 9 Contact heat transfer coefficient in dependence on the effective thermal conductivity of the solid bed.

Figure 10 shows the dependence of the contact heat transfer coefficient on the bed density. The contact heat transfer coefficient increases with the bed density. The bed density was determined by the bed porosity. A higher bed density reduces the heat penetration resistance into the solid bed thus increasing the contact heat transfer coefficient.

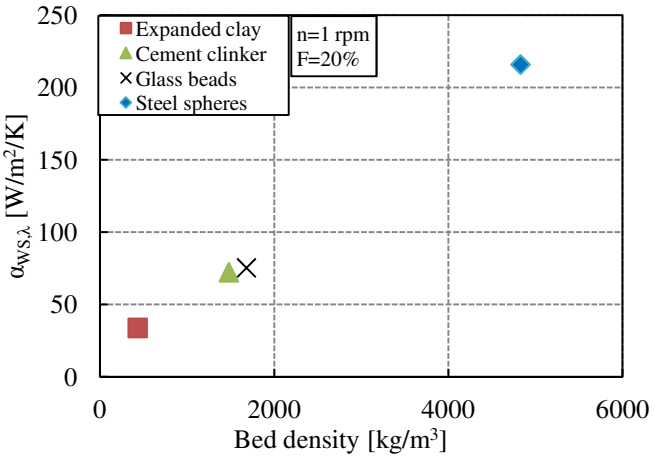

Figure 10 Contact heat transfer coefficient in dependence on the bed density.

CONCLUSION

The contact heat transfer between the wall and solid bed was experimentally investigated in an indirectly heated rotary batch drum. A monodisperse solid bed of steel spheres, animal powder, cement clinker, quartz sand, glass beads and expanded clay were used as test materials with variation in rotational speed and a constant heat flux from the heating system. It is shown that the contact heat transfer coefficient increases with higher rotational speeds. In addition, the effective thermo physical properties (density, heat capacity and thermal conductivity) have a significant influence on the contact heat transfer coefficient. When the effective thermo physical properties are higher, the contact heat transfer coefficient increases. This is due to the lower penetration resistance inside the solid bed. Furthermore, as the particle diameter increases, the contact heat transfer coefficient decreases. This is due to the higher contact resistance between the covered wall and the first particle layer of the solid bed. The measured values are compared with various model approaches from the literature. The results show good agreement between the experimental measurements and the models developed by Schlünder et al. [11] and Li et al. [7].

ACKNOWLEDGEMENT

The authors gratefully thank the German Federation of Industrial Research Associations (AiF) for funding the research project IGF-17133.

REFERENCES

[1] Ernst, R., Wärmeübertragung an Wärmetauschern im Moving Bed, *Chem. Ing. Tech*., Vol. 32, No. 1, 1960, pp. 17-22.

[2] Gorog, J.P., Adams, T.N. and Brimacombe, J.K., Regenerative heat transfer in rotary kilns, *Metall. Trans. B*, Vol. 13, No. 2, June 1982, pp. 153-163.

[3] Henein, H., Brimacombe, J.K. and Watkinson, A.P., Experimental study of transverse bed motion in rotary kilns, *Metall. Trans. B*, Vol. 14, No. 2, June 1983, pp. 191-205.

[4] Henein, H., Brimacombe, J.K. and Watkinson, A.P., The modeling of transverse solids motion in rotary kilns, *Metall. Trans. B*, Vol. 14, No. 2, June 1983, pp. 207-220.

[5] Herz, F., Mitov, I., Specht, E. and Stanev, R., Experimental study of the contact heat transfer coefficient between the covered wall and the solid bed in rotary drum, *Chemical Engineering Science*, Vol. 82, September 2012, pp. 312-318.

[6] Lehmberg, J., Hehl, M. and Schügerl, K., Transverse mixing and heat transfer in horizontal rotary drum reactors, *Powder Technol.*, Vol. 18, No. 2, November-December 1977, pp. 149-163.

[7] Li, S.-Q., Ma, L.-B., Wan, W. and Yan, Q., A mathematical model of heat transfer in a rotary kiln thermo-reactor, *Chem. Eng. Technol*., Vol. 28, No. 12, December 2005, pp. 1480-1489.

[8] Lybaert, P., Wall-particles heat transfer in rotating heat exchangers, *Int. J. Heat Mass Transfer*, Vol. 30, No. 8, August 1987, pp. 1663-1672.

[9] Schlünder, E.-U., Wärmeübergang an bewegte Kugelschüttungen bei kurzfristigem Kontakt, *Chem. Ing. Tech.*, Vol. 43, No. 11, June 1971, pp. 651-654.

[10] Schlünder, E.-U., Heat transfer to packed and stirred beds from the surface of immersed bodies, *Chem. Eng. Process.*, Vol. 18, No. 1, 1984, pp. 31-53.

[11] Schlünder, E.-U. and Mollekopf, N., Vacuum contact drying of free flowing mechanically agitated particulate material, *Chem. Eng. Process*., Vol. 18, No. 2, March-April 1984, pp. 93-111.

[12] Tscheng, S.H. and Watkinson, A.P., Convective heat transfer in a rotary kiln, *Can. J. Chem. Eng*., Vol. 57, No. 4, August 1979, pp. 433-443.

[13] Wes, G.W.J., Drinkenburg, A.A.H. and Stemerding, S., Heat transfer in a horizontal rotary drum reactor, *Powder Technol*., Vol. 13, No. 2, March-April 1976, pp. 185-192.

[14] Liu, X.Y., Specht, E., Gonzalez, O.G. and P. Walzel, Analytical solution for the rolling mode granular motion in rotary kilns, *Chem. Eng. Process*., Vol. 45, No. 6, June 2006, pp. 515-521.

[15] Mellmann, J., The transverse motion of solids in rotating cylinders-forms of motion and transition behavior, *Powder Technol*., Vol. 118, No. 3, August 2001, pp. 251-270.

[16] Wachters, L.H.J. and Kramers, H., The calcining of sodium bicarbonate in a rotary kiln, *Proceedings of 3rd European Symposium Chemical Reaction Engineering*, Vol. 77, 1964.